Comparison of Multimaterial Decomposition Fat Fraction with DECT and Proton Density Fat Fraction with IDEAL IQ MRI for Quantification of Liver Steatosis in a Population Exposed to Chemotherapy

Giuseppe Corrias[1,2], Marco Erta[2], Marcello Sini[2], Claudia Sardu[3], Luca Saba[2], Usman Mahmood[4], Sandra Huicochea Castellanos[1], David Bates[1], Nicola Mondanelli[5] ⓘ, Brian Thomsen[6], Gabriella Carollo[7], Peter Sawan[1,*], and Lorenzo Mannelli[8,*] ⓘ

Abstract

Introduction: Oncologic patients who develop chemotherapy-associated liver injury (CALI) secondary to chemotherapy treatment tend to have worse outcomes. Biopsy remains the gold standard for the diagnosis of hepatic steatosis. The purpose of this article is to compare 2 alternatives: Proton-Density-Fat-Fraction (PDFF) MRI and MultiMaterial-Decomposition (MMD) DECT.

Materials and Methods: 49 consecutive oncologic patients treated with Chemotherapy underwent abdominal DECT and abdominal MRI within 2 weeks of each other. Two radiologists tracked Regions of Interest independently both in the PDFF fat maps and in the MMD DECT fat maps. Non-parametric exact Wilcoxon signed rank test and Cohen's K were used to compare the 2 sequences and to evaluate the agreement.

Results: There was no statistically significant difference in the fat fraction measured as a continuous value between PDFF and DECT between 2 readers. Within the same imaging method (PDFF) the degree of agreement based on the k coefficient between reader 1 and reader 2 is 0.88 (p-value < 0.05). Similarly, for single-source DECT(ssDECT) the degree of agreement based on the k coefficient between reader 1 and reader 2 is 0.97 (p-value < 0.05).

Conclusions: The results of this study demonstrate that the hepatic fat fraction of ssDECT with MMD are not significantly different from PDFF. This could be an advantage in an oncological population that undergoes serial CT scans for follow up of chemotherapy response.

[1] Department of Radiology, Memorial Sloan Kettering Cancer Center, New York, NY, USA
[2] Department of Radiology, University of Cagliari, Italy
[3] Department of Medical Science, University of Cagliari, Italy
[4] Department of Medical Physics, Memorial Sloan Kettering Cancer Center, New York, NY, USA
[5] Orthopedics and Traumatology, University of Siena, Italy
[6] GE Healthcare, Chicago, Illinois.
[7] St. John's University, Jamaica, NY, USA
[8] IRCCS SDN, Napoli, Italy
* Peter Sawan and Lorenzo Mannelli have contributed equally.

Corresponding Authors:
Lorenzo Mannelli, IRCCS SDN, Naples, Italy.
Email: mannellilorenzo@yahoo.it

Peter Sawan, Department of Radiology, Memorial Sloan Kettering Cancer Center, New York, NY, USA.
Email: sawanp@mskcc.org

Introduction

Among the currently available treatment options for patients with cancer, conventional chemotherapy is one of the most effective and widely used. The side effects of chemotherapy are well known, and the liver, with its rich blood supply and key role in processing metabolites, can be at risk for cytotoxic injury.[1,2] Chemotherapy-associated liver injury (CALI) is a specific form of steatohepatitis that may occur in cancer patients treated with chemotherapy. CALI is divided in 2 groups (fatty liver spectrum and sinusoidal injuries). On the fatty liver side, outcomes are different between simple steatosis and nonalcoholic steatohepatitis (NASH). CALI has different patterns for development of steatohepatitis that are the result of typical cellular hepatic lesions: vascular damage, necrosis, fibrosis, and cholestasis, following steps similar to non-alcoholic fatty liver disease (NAFLD).[1,3-5]

Patients who develop CALI secondary to chemotherapy treatment tend to have worse outcomes,[5] since they could need to stop or modulate the chemotherapy regimen. Furthermore, steatosis is a risk factor in the oncological population treated with chemotherapy but also patients undergoing major hepatectomies since it increases post-surgery mortality and morbidity. An objective and non-invasive method to evaluate the extent of CALI and to differentiate the normal accumulation of fat in induced steatohepatitis from prior steatohepatitis is essential to patient overall survival.[6] Biopsy remains the gold standard for the diagnosis of hepatic steatosis, however its invasive nature limits its use in daily clinical practice. When evaluating hepatic steatosis, the limitations with CT include the low sensitivity for mild to moderate steatosis and multiple confounding factors (presence of iron, fibrosis, edema) that do not allow a precise assessment of liver fat, especially in liver donors.[7] The dose of ionizing radiation administered to the patient is also of concern, but with modern CT technical advances, such as automated tube current modulation, the risk to the patient is significantly reduced. MR imaging is one of the most used methods for detection and characterization of hepatic steatosis.

Recently, quantitative confounder-corrected, chemical-shift-encoded (CSE) MRI sequences have emerged as methods capable of quantifying liver proton density fat fraction (PDFF). PDFF has been demonstrated as being a standardized, reproducible and promising biomarker for the quantification of hepatic steatosis.[8] It is increasingly considered as a viable alternative to biopsy for certain cohorts of patients, as in the case of patients who received chemotherapy and require continuous monitoring of liver function.[8,9]

One commercial implementation of CSE-MRI is Iterative Decomposition of water and fat with Echo Asymmetry and Least squares estimation (IDEAL-IQ), a novel MRI technique that is highly precise and accurate for quantifying PDFF as a biomarker of hepatic steatosis.[10,11] In IDEAL-IQ, images are acquired at multiple echo times, and an iterative least-squares decomposition algorithm is employed to simultaneous solve for an iron-corrected PDFF map and a fat-corrected R2* ($=1/T2*$) map. By incorporating a field map variable into the algorithm, IDEAL-IQ accounts for T2* effects/field inhomogeneity and yields estimates of PDFF not-confounded by iron overload. Thus IDEAL-IQ presents a more sophisticated fat quantification approach that corrects for the confounding factors of in phase / out of phase imaging (IOP) outlined above. IDEAL-IQ has already been validated experimentally, in phantoms and in mice, and clinically, in patients with nonalcoholic fatty liver disease.[10,12] More recently, research efforts have shown that IDEAL-IQ can reliably quantify fat fraction in patients with iron overload.[13] However, IDEAL-IQ has yet to be tested in an oncologic population at risk for CALI.

In recent years, the dual-energy CT (DECT) has been increasingly used for the evaluation of fat distribution within liver and breast.[14] DECT, which uses 2 different tube voltages (generally 140 and 80 kVp), may be used to evaluate and delineate the focal and diffuse fatty infiltration of the liver by measuring the change in hepatic attenuation between images acquired at the low and high tube voltages.[14-18] The latest DECT based multimaterial decomposition algorithm (MMD)[17,18] allows quantification of the percentage of fat in a volume of tissue. The MMD also has the advantage of enabling one to quantify the fat content of the liver in both contrast- and non-contrast enhanced data sets.[19] Since CT is the most widely used imaging method for tumor staging and patient follow up, and since several of the latest CT systems are being deployed with DECT capabilities, this new approach presents an opportunity to objectively monitor patients undergoing chemotherapy and who may be susceptible to liver related adverse effects.[14]

Patients who undergo chemotherapy should be evaluated with multiple serial imaging exams to evaluate the effectiveness of the therapy. In this context DECT could allow a simultaneous assessment of the accumulation of hepatic fat and the follow up of the cancer patient, allowing an optimization in time and most importantly economic resources.

The objective of this study is to assess the correlation and compare reader agreement and reproducibility in the quantification of hepatic steatosis between CSE-MRI and DECT based MMD in an oncologic patient population undergoing chemotherapy treatment.

Materials and Methods

Study Population

This retrospective study was approved by the institutional review board with a waiver of informed consent. The study population consisted of 49 consecutive patients. Patients were
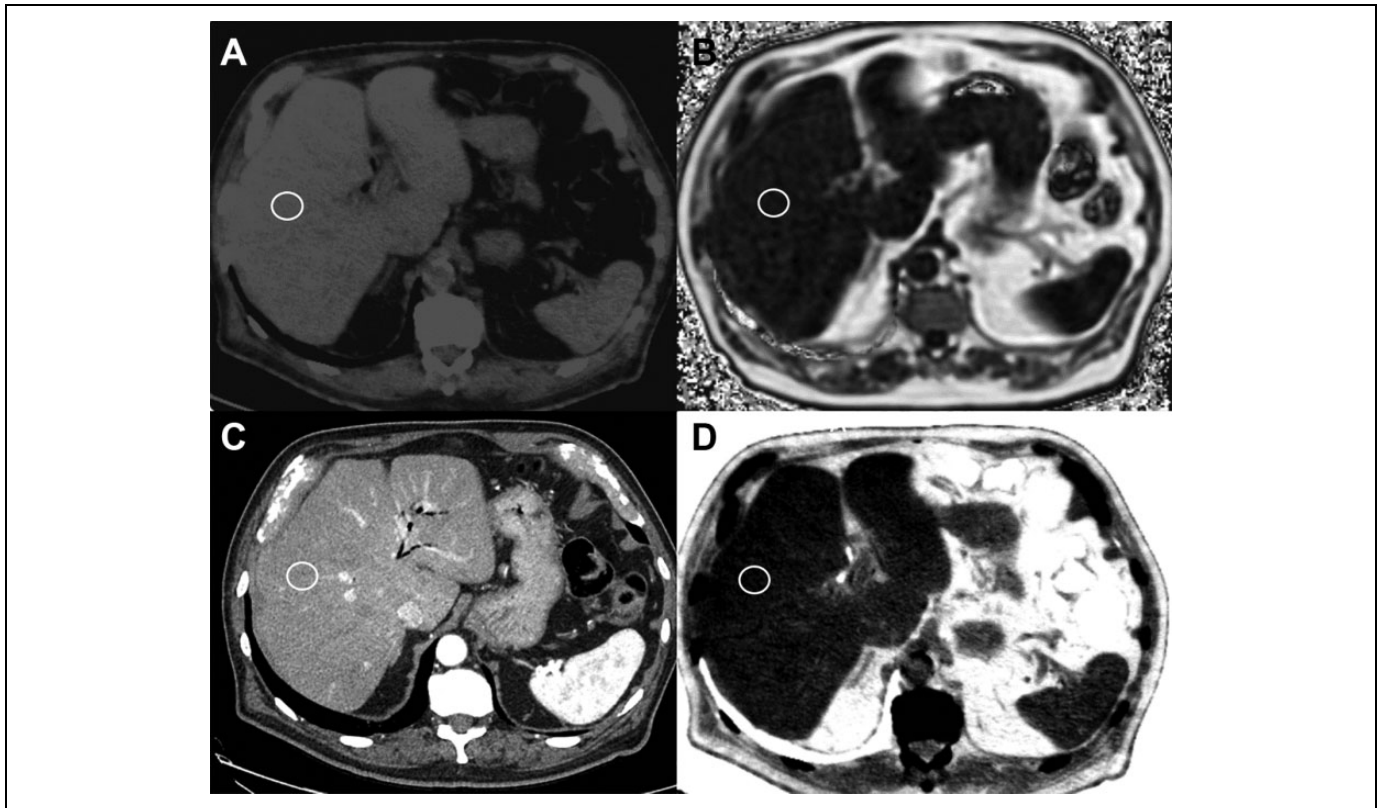
Figure 1. 80-years-old male with bladder cancer patient with no known steatosis. ROIs traced in the right liver, avoiding major vessels and bile ducts. A) MRI IDEAL IQ sequence, R2* \ IRON map shows that there is no evidence of iron surcharge (R2* = 122.08). B) MRI IDEAL IQ sequence, PDFF map shows no evidence of steatosis: PDFF = 3.3% normal values < 6.6%. C) Monochromatic DECT at 60keV. The placed ROI at the level of the VI hepatic segment shows an HU of 85. D) FVF map. An ROI placed in the same point as in C gives back a calculated FVF of 5.5%.

selected into the institutional database, looking for patients which underwent upper abdominal DECT with kVp switching and upper abdominal MRI within 2 weeks of each other. The studies were performed at a tertiary oncologic center between March and June 2017, for different clinical indications. All patients had been previously diagnosed with any type of cancer. All patients underwent at least 2 cycles of Cht before being scanned. The maximum interval between the last cycle of Cht and the exams was set to be 6 weeks. Only liver MRI exams with T1-weightened-in-phase (IP) out-of-phase (OP) and CSE-MRI acquisitions were included in the study.

Exclusion criteria included: patients BMI > 25 and patients with metabolic syndrome, in order to eliminate confusing factors for steatosis appearance; patients with known widespread metastatic disease, viral hepatitis, cholestasis; poor image quality (evaluated in conjunction by both radiologists).

The study was carried out by 2 radiologists, both with 4 years of experience, who tracked their ROIs independently. The readers were blinded and they both performed the MRI and DECT measurements.

MR Imaging Parameters

All studies were performed on a 1.5 T MRI imaging system (OptimaMR450w, GE Healthcare, Waukesha, WI) with a 32

Channel Torso Array Coil. The protocol included: 1) CSE-MRI (IDEAL IQ, GE Healthcare, Waukesha, WI) to produce simultaneous iron-corrected PDFF and fat-corrected R2* maps; 2) IP/OP MRI. Acquisition parameters for IDEAL IQ were as follows: single breath hold acquisition lasting less than 30 seconds (average 21 seconds), TR 10 ms, TE variable, FOV 35-40 cm, matrix 128 x 128, pixel bandwidth 395 kHz, flip angle 6°, slice thickness 10 mm, and space between slices 5 mm. We acquired 6 different echoes ranging from 1.1 ms to 6.38 ms. Post processing was performed with a software provided by the manufacturer to create PDFF maps (Figures 1 and 2). Acquisition parameters for IP/OP T1 were as follow: single breath hold acquisition lasting 15 seconds, TR: 150 ms, out-of-phase TE 2.115 ms, in-phase TE: 4.252, FOV: 35-40 cm, matrix 320x192, slice thickness 7 mm, space between slices 1 mm. All ROIs were placed in the liver avoiding major vessels, ligaments and bile ducts, making sure that each ROI was surrounded by liver parenchyma. 3 ROIs (2 cm of diameter) per patient were positioned in segment 2/3, segment 5 and segment 6. The ROIs were drawn in the chemical shift sequence and copy and paste in the fat-fraction map. In order not to lose any signal intensity due to different distances from the receiving coil, and to uniform the objectivity of positioning, all ROIs where drawn at the same distance from the coil isocenter: ROIs were drawn inside of a circular band extending from 10 to 15
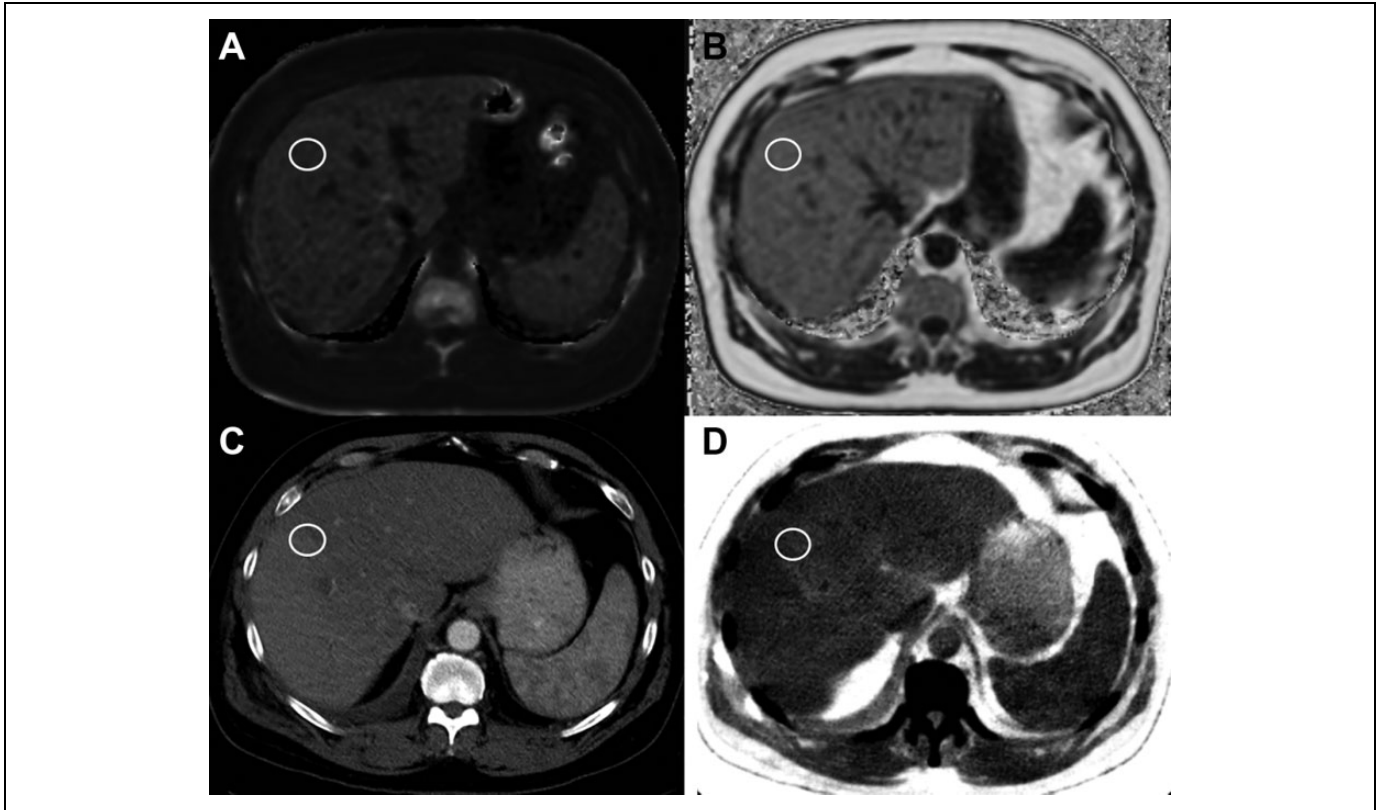
Figure 2. 59-years-old male with colon cancer. Steatosis. ROIs traced in the right liver, avoiding major vessels and bile ducts. A) MRI IDEAL IQ sequence, R2* \ IRON map shows that there is no evidence of iron surcharge (R2* = 123). B) MRI IDEAL IQ sequence, PDFF map shows evidence of advanced steatosis: PDFF = 36.2% normal values < 6.6%. C) Monochromatic DECT at 60keV. The placed ROI at the level of the VIII hepatic segment shows an HU of 85. D) FVF map. An ROI placed in the same point as in C gives back a calculated FVF of 20%.

cm from the isocenter, according to the anatomic landmark specified above. The fat fraction was calculated from IP/OP imaging and measured from IDEAL-IQ fat fraction maps.

DECT Image Parameters

Abdominal CT scans were performed using a single source DECT (ssDECT) scanner (GE Discovery CT750 HD, GE Healthcare, Milwaukee, Wisconsin). A triphasic liver protocol was used on all patients: after an unenhanced phase, the late arterial and venous phase images were acquired at 40s and 80s following the intravenous administration of 150 mL of iodinated contrast material at 4 mL/s (Iohexol 300 mgI/mL, Omnipaque 300, GE Healthcare, Cork, Ireland), respectively. The late arterial phase was acquired by using the Gemstone Spectral imaging, ssDECT (GSI, GE Healthcare, Milwaukee, Wisconsin) modality: fast switching voltage 80/140 kVp, fixed mA, 0.7 s rotation time, pitch 0.984. Images were reconstructed with a matrix of 512x512, standard deconvolution kernel, and a thickness of 2.5 mm spaced by 2.5 mm.

Two radiologists (GC and RG) reconstructed the ssDECT late arterial phase datasets with GSI Volume Viewer on Advantage volume share 7 (GE Healthcare, Milwaukee, Wisconsin) to obtain monochromatic images at 60 keV and material

density fat (MMD-FAT) images (Figure 1). 3 ROIs per patient where placed as described in the MRI section.

As noted in Figures 1 and 2, MMD-FAT images display the fat volume fraction (FVF) in percentage.

Statistics

The collected variables were tested for normality with Kolmogorov-Smirnov Test and with the Shapiro-Wilk Test (Tables 1 and 2).

Thereafter, the first approach considered the variables as continuous, and compared them with non-parametric exact Wilcoxon signed rank test, since all the data had a non-gaussian distribution. The second approach divided the fat-content continuous variable into 3 categories according to the fat content of the liver, using cutoffs, as it has already been done in literature. We used literature-based proposed hepatic fat fraction (HFF) intervals for each histological steatosis grade in nonalcoholic fatty liver disease are: 0–6.4% for grade 0 (normal); 6.5–17.4% for grade 1 (mild); 17.5–22.1% for grade 2 (moderate); and 22.2% or greater for grade 3 (severe).[20]

Intraclass correlation coefficient (ICC) was used to assess the degree of intra-reader and inter-reader agreement in the quantification of hepatic fat by imaging acquired through IDEAL-IQ and ssDECT. Bland-Altman difference plots with

Table 1. Variables were tested for normality with Kolmogorov-Smirnov Test and with the Shapiro-Wilk Test. Both tests show that variables are continually distributed.

| | | Reader 1 | | | | | | | Reader 2 | | | | | |
| | | Kolmogorov-Smirnov[a] | | | Shapiro-Wilk | | | | Kolmogorov-Smirnov[a] | | | Shapiro-Wilk | | |
		Statistic	df	Sig.	Statistic	df	Sig.		Statistic	df	Sig.	Statistic	df	Sig.
IDEAL IQ	Liver S6	0.336	39	0.000	0.647	39	0.000	Liver S6	0.353	39	0.000	0.634	39	0.000
	Liver S5	0.349	39	0.000	0.630	39	0.000	Liver S5	0.350	39	0.000	0.635	39	0.000
	Liver S2/3	0.339	39	0.000	0.647	39	0.000	Liver S2/3	0.339	39	0.000	0.638	39	0.000
DECT	Liver S6	0.350	39	0.000	0.654	39	0.000	Liver S6	0.375	39	0.000	0.660	39	0.000
	Liver S5	0.330	39	0.000	0.650	39	0.000	Liver S5	0.346	39	0.000	0.655	39	0.000
	Liver S2/3	0.312	39	0.000	0.663	39	0.000	Liver S2/3	0.328	39	0.000	0.659	39	0.000
	a. Lilliefors Significance Correction							a. Lilliefors Significance Correction						

Table 2. Variables were tested for normality with Kolmogorov-Smirnov Test and with the Shapiro-Wilk Test. Both tests show that variables are continually distributed.

| Reader 1 | | | | Reader 2 | | | |
	S6	S5	S2/3		S6	S5	S2/3
Z	-1,516[b]	-,783[b]	-,434[b]	Z	-1,138[b]	-,990[b]	-2,692[b]
Asymp. Sig. (2-tailed)	0.130	0.434	0.665	Asymp. Sig. (2-tailed)	0.255	0.322	0.199

multiple measurements per subject were also used to assess agreement and bias among PDFF measurements across readers and to assess agreement and bias among different techniques.

ICC values were interpreted as follows Values less than 0.5 are indicative of poor reliability, values between 0.5 and 0.75 indicate moderate reliability, values between 0.75 and 0.9 indicate good reliability, and values greater than 0.90 indicate excellent reliability. A test with a p-value <0.05 was considered statistically significant.[21]

Results

A total of 49 consecutive oncological patients were considered for the study. Five patients were excluded due to poor image quality, specifically on the IDEAL-IQ sequence, where motion artifacts were prevalent. Patients with known liver metastatic disease (2 patients), viral hepatitis (1 patients), cholestasis (2 patients) were excluded from the study. The final patient population consisted of 39 patients (20 males, 19 females), mean age 59 years (M = 65; F = 57).

Fat content findings are summarized for different readers and techniques in Table 3. Based on the thresholds given in the materials and methods, reader 1 found an increased fat fraction (>6.5%) in 18 patients (62%) with ssDECT and in 20 patients (69%) in IDEAL-IQ; reader 2 found an increased fat fraction (>6.5%) in 20 patients (69%) with both DECT and IDEAL-IQ.

There was no statistically significant difference (Wilcoxon Signed-Rank test) in the fat fraction measured as a continuous

Table 3. Fat content findings summarized for different readers and techniques.

| Reader 1 | DECT Steatosis grade | | | | |
IQ steatosis grade	0	1	2	3	Total
0	8	1	0	0	9
1	3	12	0	0	15
2	0	0	13	1	14
3	0	0	0	1	1
Total	11	13	3	2	39
READER 2					
0	7	3	0	0	10
1	3	11	0	0	14
2	0	0	13	0	13
3	0	0	0	2	2
	10	14	3	2	39

value (FF%) between IDEAL-IQ and DECT for reader 1 (Table 4) and for reader 2 (Table 5). Within the same imaging method (IDEAL IQ) the degree of agreement for FF% based on the k coefficient between reader 1 and reader 2 is 0.88 (p value <0.05). Similarly, for ssDECT the degree of agreement based on the k coefficient between reader 1 and reader 2 is 0.97 (p value <0.05).

The degree of overall intra-reader agreement was evaluated on the results produced by the 2 methods (IDEAL IQ and ssDECT). The analysis of agreement with the ICC showed an agreement of 0.85 (p value <0.05) for Reader 1and of 0.84 (p value <0.05) for Reader 2.

Table 4. No statistically significant difference was found in the fat fraction measured as a continuous value between IDEAL-IQ and DECT for reader 1, tested with Wilcoxon Signed Ranks Test and for reader 1.

Reader 1. Wilcoxon signed ranks test			
	Liver S6–Liver S6	Liver S5–Liver S5	Liver S2/3–Liver S2/3
Z	-1,138[b]	-,990[b]	-2,692[b]
Asymp. Sig. (2-tailed)	,255	,322	,007

a. Wilcoxon Signed Ranks Test.

Table 5. No statistically significant difference was found in the fat fraction measured as a continuous value between IDEAL-IQ and DECT for reader 1, tested with Wilcoxon Signed Ranks Test and for reader 2.

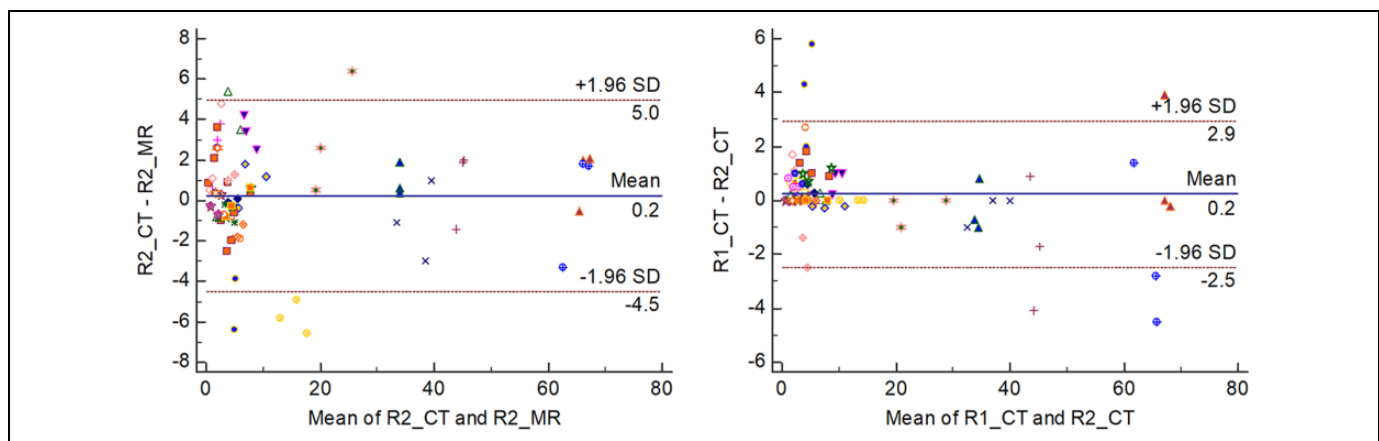| Reader 2. Wilcoxon signed ranks test			
	Liver S6–Liver S6	Liver S5–Liver S5	Liver S2/3–Liver S2/3
Z	-1,516[b]	-,783[b]	-,434[b]
Asymp. Sig. (2-tailed)	,130	,434	,665

a. Wilcoxon Signed Ranks Test.

Figure 3. Bland-Altman difference plots for fat fraction measurements generated by using PDFF MRI and material decomposition dsDECT and analyzed by 2 different readers blinded to each other's findings. Each different symbol is a different patient. Dotted red lines demarcate 1.96 standard deviations (SD).

Bland-Altman analysis according to individual reader showed only very slight mean biases between the various imaging techniques (Figure 3): CT vs MRI reader 1 0.6% and CT vs MRI reader 2 0.22%.

Discussion

The results of this study demonstrate that the hepatic fat fraction (HFF) of DECT with MMD are not significantly different from PDFF obtained with IDEAL IQ.

To the best of our knowledge, this is the first study to focus on comparing HFF assessment between imaging modalities in an oncologic population. The importance of this finding is that oncologic patients undergo multiple CT scans to monitor the primary disease and/or for monitoring the presence of liver fat before, during and after treatment with chemotherapy. It is not conceivable that in a clinical setting, patients would receive multiple liver biopsies only to control the onset of CALI. Finding a single imaging modality that could quantify HFF during staging scans performed in a single acquisition has the potential to help in objectively evaluating hepatic function and HFF will reduce errors associated with subjective image interpretation, reduce the time spent by patients in the clinic and potentially improve patient outcomes.

US, CT and MR imaging are all useful imaging modalities for detecting the presence of hepatic fat content and indirectly hepatocellular injury. Although MRI imaging techniques are considered to be more precise for quantifying hepatic steatosis, our study suggests that DECT based fat quantification may be another useful tool, perhaps comparable to the recently developed CSE-MRI method.[22-24] DECT is also more effective in allowing correction of beam irradiation, and for this reason the

MMD technique may be less influenced by body size compared to single-energy CT.[19,25-27]

Some patients with increased fat content progress to cirrhosis and hepatocellular carcinoma. DECT allows the discrimination of substance using monochromatic image (MI), and steatosis exhibit specifically the CT value of each energy level.[28,29] Recently an algorithm for the evaluation of liver fibrosis with DECT has been successfully implemented with a good correlation with Magnetic Resonance Elastography (MRE).[30] MRE is at the moment the most reliable, not invasive, available method to evaluate liver fibrosis.[31] However, in our cohort 5 patients out of 39 (12.8%) were exclude due to motion artifacts during the MRI examinations. This could be a limitation of MRI, especially in an oncological population, using a technique such as CSE-MRI for which patients are asked to hold their breath for about 30 seconds. Ultimately, new MR and DECT techniques consent to analyze the hepatic iron content.[32,33] Soon, hepatic disease in a cirrhotic patient or in an oncological patient at risk for hepatic metastasis, would be ideally evaluated with an all-encompassing CT or MR study, including arterial and portal phase for evaluation of HCC nodules but also studying HFF, liver fibrosis and iron content. This would allow the implementation of a so-called digital liver biopsy with CT or MR.[34]

A future implementation could also be the radiomic analysis of these quantitative hepatic characteristics (i.e. HFF, Iron content, Fibrosis); each of these could be heterogeneously distributed in the liver, and a random sampling with ROIs could be misleading to an accurate evaluation. Segmentation of the whole liver by artificial intelligence, and thorough radiomic analysis of HFF, Iron content, Fibrosis, would ideally indicate which areas of the liver have disease and may be an indicator of progression to HCC in this specific area. Texture analysis of the whole liver has been evaluated by some authors to assess preoperative risk stratification in patients candidates to hepatic surgery exposed to liver insufficiency.[35]

This study has several limitations. First, none of the patients had liver biopsy: the sensitivity and specificity of PDFF for establishing the diagnosis is not 100%: the PDFF threshold of 6.4% to diagnose grade 1 or higher steatosis had 86% sensitivity and 83% specificity; the threshold of 17.4% to diagnose grade 2 or higher steatosis had 64% sensitivity and 96% specificity, and the threshold of 22.1% to diagnose grade 3 steatosis had 71% sensitivity and 92% specificity. Secondly, the population with normal HFF was relatively small compared to the distribution of this disease among the general population (38% for Reader 1, 31% for Reader 2). However, this is a typical distribution for an oncological population exposed to chemotherapy. Thirdly, the absolute gold standard in evaluating hepatic steatosis is the pathological specimen, since it provides not only an evaluation of liver fat but also fibrosis, iron content and hepatic micro-architecture; our study did not have any pathological gold standard, since in a oncological population, liver biopsies for analyzing hepatic functionality are not part of the current good clinical practice. And finally, from an imaging perspective, MRI-PDFF and DECT FVF are imaging biomarkers of liver fat, that are similar, but not identical. MRI measurements are based on the fraction of mobile protons in the liver attributable to fat, whereas MMD DECT analyzes photons attenuation data under predetermined assumptions of material composition. Also, each technique is differently affected by the presence of other tissue properties and materials within a given voxel.

In conclusion, the quantification of HFF using post-contrast DECT correlates with PDFF analyzed with IDEAL IQ. Both methods have excellent inter-reader agreement. Furthermore, in our small patient cohort we had to exclude 5 patients because of movement artifacts during MRI acquisition; this could be a potential advantage of DECT.

Key points

- HFFs of ssDECT with MMD are not significantly different from PDFF obtained with IDEAL IQ.
- The agreement between readers is good for both techniques.
- This could be an advantage in an oncological population that undergoes seriate CT scans for follow up of chemotherapy response, since CT follow up scans are routinely performed in this population, who can benefit of a timely diagnosis of CALI.

Abbreviations

CALI: chemotherapy-associated liver injury; NAFLD: non-alcoholic fatty liver disease; CSE: chemical-shift-encoded MRI; PDFF: proton density fat fraction; DECT: dual-energy CT; IDEAL-IQ: Iterative Decomposition of water and fat with Echo Asymmetry and Least squares estimation; MMD: multimaterial decomposition algorithm; HFF: hepatic fat fraction; Cht: Chemotherapy.

Authors' Note

Lorenzo Mannelli and Peter Sawan are equally contributed to this manuscript. The authors were equally involved in acquisition of data, analysis and interpretation of data, drafting of the manuscript, critical revision of the manuscript for important intellectual content, statistical analysis, technical, or material support of this study. Our institutional review board approved the study with a waiver for informed consents.

ORCID iD

Nicola Mondanelli ⬤ https://orcid.org/0000-0002-0684-4197
Lorenzo Mannelli ⬤ https://orcid.org/0000-0002-9102-4176

References

1. Maor Y, Malnick S. Liver injury induced by anticancer chemotherapy and radiation therapy. *Int J Hepatol*. 2013. doi:10.1155/2013/815105

2. Grigorian A, O'Brien CB. Hepatotoxicity secondary to chemotherapy. *J Clin Transl Hepatol*. 2014;2:95-102.

3. Thatishetty AV, Agresti N, O'Brien CB. Chemotherapy-induced hepatotoxicity. *Clin Liver Dis*. 2013;17:671–686, ix-x.

4. King PD, Perry MC. Hepatotoxicity of chemotherapy. *The Oncologist*. 2001;6:162-176.

5. Stravitz RT, Sanyal AJ. Drug-induced steatohepatitis. *Clin Liver Dis*. 2003;7:435-451.

6. Schwarz RE, Berlin JD, Lenz HJ, Nordlinger B, Rubbia-Brandt L, Choti MA. Systemic cytotoxic and biological therapies of colorectal liver metastases: expert consensus statement. *HPB*. 2013;15:106-115.

7. Limanond P, Raman SS, Lassman C, et al. Macrovesicular hepatic steatosis in living related liver donors: correlation between CT and histologic findings. *Radiology*. 2004;230:276-280.

8. Kukuk GM, Hittatiya K, Sprinkart AM, et al. Comparison between modified Dixon MRI techniques, MR spectroscopic relaxometry, and different histologic quantification methods in the assessment of hepatic steatosis. *Eur Radiol*. 2015;25:2869-2879.

9. Tang A, Desai A, Hamilton G, et al. Accuracy of MR imaging-estimated proton density fat fraction for classification of dichotomized histologic steatosis grades in nonalcoholic fatty liver disease. *Radiology*. 2015;274:416-425.

10. Idilman IS, Aniktar H, Idilman R, et al. Hepatic steatosis: quantification by proton density fat fraction with MR imaging versus liver biopsy. *Radiology*. 2013;267:767-775.

11. Chiang H-J, Lin L-H, Li C-W, et al. Magnetic resonance fat quantification in living donor liver transplantation. *Transplant Proc*. 2014;46:666-668.

12. Idilman IS, Tuzun A, Savas B, et al. Quantification of liver, pancreas, kidney, and vertebral body MRI-PDFF in non-alcoholic fatty liver disease. *Abdom Imaging*. 2015;40:1512-1519.

13. Horng DE, Hernando D, Reeder SB. Quantification of liver fat in the presence of iron overload. *J Magn Reson Imaging*. 2017;45:428-439.

14. Sun T, Lin X, Chen K. Evaluation of hepatic steatosis using dual-energy CT with MR comparison. *Front Biosci Landmark Ed*. 2014;19:1377-1385.

15. Ma X, Holalkere N-S, Kambadakone RA, Mino-Kenudson M, Hahn PF, Sahani DV. Imaging-based quantification of hepatic fat: methods and clinical applications. *Radiogr Rev Publ Radiol Soc N Am Inc*. 2009;29:1253-1277.

16. Raptopoulos V, Karellas A, Bernstein J, Reale FR, Constantinou C, Zawacki JK. Value of dual-energy CT in differentiating focal fatty infiltration of the liver from low-density masses. *Am J Roentgenol*. 1991;157:721-725.

17. Mendler M-H, Bouillet P, Le Sidaner A, et al. Dual-energy CT in the diagnosis and quantification of fatty liver: limited clinical value in comparison to ultrasound scan and single-energy CT, with special reference to iron overload. *J Hepatol*. 1998;28:785-794.

18. Li J-H, Tsai C-Y, Huang H-M. Assessment of hepatic fatty infiltration using dual-energy computed tomography: a phantom study. *Physiol Meas*. 2014;35:597-606.

19. Hyodo T, Yada N, Hori M, et al. Multimaterial decomposition algorithm for the quantification of liver fat content by using fast-kilovolt-peak switching dual-energy CT: clinical evaluation. *Radiology*. 2017;283:108-118.

20. Szczepaniak LS, Nurenberg P, Leonard D, et al. Magnetic resonance spectroscopy to measure hepatic triglyceride content: prevalence of hepatic steatosis in the general population. *Am J Physiol Endocrinol Metab*. 2005;288:E462-E468.

21. Landis JR, Koch GG. The measurement of observer agreement for categorical data. *Biometrics*. 1977;33:159-174.

22. Hur BY, Lee JM, Hyunsik W, et al. Quantification of the fat fraction in the liver using dual-energy computed tomography and multimaterial decomposition. *J Comput Assist Tomogr*. 2014;38:845-852.

23. Corrias G, Krebs S, Eskreis-Winkler S, et al. MRI liver fat quantification in an oncologic population: the added value of complex chemical shift-encoded MRI. *Clin Imaging*. 2018;52:193-199.

24. Aoki T, Yamaguchi S, Kinoshita S, Hayashida Y, Korogi Y. Quantification of bone marrow fat content using iterative decomposition of water and fat with echo asymmetry and least-squares estimation (IDEAL): reproducibility, site variation and correlation with age and menopause. *Br J Radiol*. 2016;89. doi: 10.1259/bjr.20150538

25. Hyodo T, Hori M, Lamb P, et al. Multimaterial decomposition algorithm for the quantification of liver fat content by using fast-kilovolt-peak switching dual-energy CT: experimental validation. *Radiology*. 2016;282:381-389.

26. Mendonça PRS, Lamb P, Sahani DV. A flexible method for multi-material decomposition of dual-energy CT images. *IEEE Trans Med Imaging*. 2014;33:99-116.

27. Yu L, Leng S, McCollough CH. Dual-energy CT–based monochromatic imaging. *Am J Roentgenol*. 2012;199:S9-S15.

28. Shuman WP, Green DE, Busey JM, et al. Dual-energy liver CT: effect of monochromatic imaging on lesion detection, conspicuity, and contrast-to-noise ratio of hypervascular lesions on late arterial phase. *AJR Am J Roentgenol*. 2014;203:601-606.

29. Okada M, Kim T, Murakami T. Hepatocellular nodules in liver cirrhosis: state of the art CT evaluation (perfusion CT/volume helical shuttle scan/dual-energy CT, etc.). *Abdom Imaging*. 2011;36:273-281.

30. Lamb P, Sahani DV, Fuentes-Orrego JM, Patino M, Ghosh A, Mendonça PRS. Stratification of patients with liver fibrosis using dual-energy CT. *IEEE Trans Med. Imaging*. 2015;34:807-815.

31. Mariappan YK, Glaser KJ, Ehman RL. Magnetic resonance elastography: a review. *Clin Anat*. 2010;23:497-511.

32. Hernando D, Levin YS, Sirlin CB, Reeder SB. Quantification of liver iron with MRI: state of the art and remaining challenges. *J Magn Reson Imaging*. 2014;40:1003-1021.

33. Ma J, Song Z-Q, Yan F-H. Separation of hepatic iron and fat by dual-source dual-energy computed tomography based on material decomposition: an animal study. *PLoS One*. 2014;9: e110964.

34. Mancini M, Summers P, Faita F, et al. Digital liver biopsy: bio-imaging of fatty liver for translational and clinical research. *World J Hepatol*. 2018;10:231-245.

35. Simpson AL, Adams LB, Allen PJ, et al. Texture analysis of preoperative CT images for prediction of postoperative hepatic insufficiency: a preliminary study. *J Am Coll Surg*. 2015;220: 339-346.